Maskless, fast and highly selective etching of fused silica with gaseous fluorine and gaseous hydrogen fluoride

Francesco Venturini[1,2,4], **Rebeca Martinez Vazquez**[3], **Roberto Osellame**[3], **Giulio Cerullo**[3], **Maurizio Sansotera**[1,2] **and Walter Navarrini**[1,2]

[1] Dipartimento di Chimica, Materiali e Ingegneria Chimica 'Giulio Natta', Politecnico di Milano, Via Luigi Mancinelli, 7, I-20133 Milan, Italy

[2] Consorzio Interuniversitario Nazionale per la Scienza e la Tecnologia dei Materiali, Via G. Giusti, 9, I-50121 Firenze, Italy

[3] Istituto di Fotonica e Nanotecnologie - CNR, Dipartimento di Fisica - Politecnico di Milano, Piazza Leonardo da Vinci, 32, I-20133 Milan, Italy

4 Author to whom any correspondence should be addressed.

E-mail: francesco.venturini@chem.polimi.it

Received 17 September 2013, revised 19 November 2013
Accepted for publication 20 November 2013
Published 23 December 2013

Introduction

Microfluidic devices are interesting tools for synthetic chemistry and analysis. They are manufactured using different substrate materials, such as metal, ceramics, glass, silicon or polymers. The choice of the material is based on the characteristics of the chemicals to be fluxed inside the microdevices. Inorganic fluorides require metal microdevices [1], organic chemicals and water-based solutions are better handled with glass devices, while polymer engraved microdevices are used because of their mechanical flexibility [2], surface energy tuning and optical properties [3–5].

Any material used in microfabrication requires its own specific machining technique. The history of micromachining is tied to the development of integrated electronic circuit technology [6]. The silicon slab needs to be covered with glass in order to obtain a working microfluidic device. In this procedure, glass is relegated as a top seal for silicon chips. This is due to the fact that, as opposed to silicon, the etching of glass is isotropic; therefore, the SiO_2 lab-on-chip devices are fabricated by means of photolithography only with planar geometries. However, when compared to silicon, glass has a lower cost, good transparency and good corrosion resistance. Thus, it remains a good candidate for being used as a main substrate in microfluidic devices, assuming that a better control of the aspect ratio of the etched channels is possible. To overcome the glass isotropic etching limitations, standard photolithographic techniques have been employed and photo-sensitive glasses have also been developed [2]. The possibility of locally modifying the glass structure

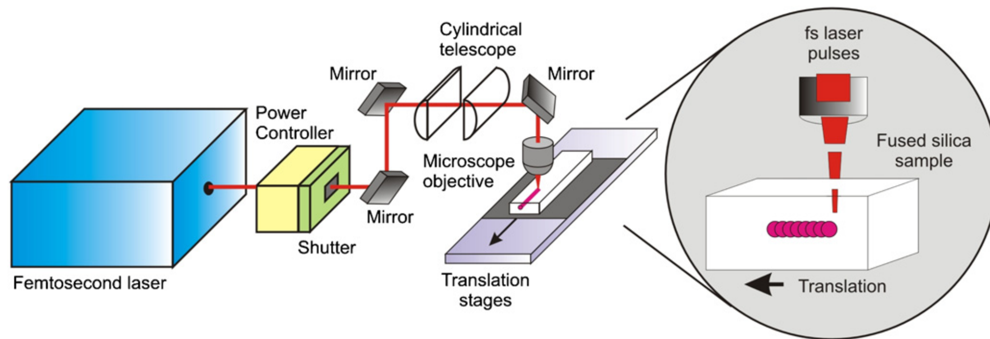

Figure 1. Setup used for femtosecond laser irradiation.

is under investigation by increasing its reactivity against etching agents via femtosecond laser irradiation followed by chemical etching (FLICE) [7–11]. With this technique, it is possible to produce three-dimensional microchannels, chambers and complex structures inside fused silica substrates. The procedure described in the literature consists in a focused laser irradiation of the silica slab followed by chemical etching using hydrofluoric acid (HF), either in the aqueous [12–14] or gas phase [15, 16]. The photomodification is executed by irradiating the transparent material placed on a motorized translation stage by a train of pulses of a focused femtosecond laser beam. In the standard approach, the subsequent selective etching is carried out by immersing the irradiated glass slab in aqueous HF or potassium hydroxide for a specified period of time. With aqueous HF, the etching process is diffusion-limited and self-terminating, leading to a maximum microchannel length of about 1.5 mm with a limited length/diameter aspect ratio; with aqueous potassium hydroxide the etching process is very slow but does not show self-termination [14].

Moreover, the etching agents so far developed (buffered oxide etch, HF/methanol, Cl_2/UV, O_3/H_2O/HF, HF-organics, SCO_2, cryogenic aerosols, NF_3 . . .) do not seem to solve the problem presented herein [17–20].

To overcome these limitations, we have recently introduced a gaseous HF implementation of the FLICE technique obtaining an aspect ratio higher than 30 [16] and a self-terminating length in excess of 3 mm [15].

The etching kinetics, the aspect ratio and the self-terminating length obtained show that the use of gaseous hydrogen fluoride has reached its limits. In particular, the water produced in the microchannel is tightly bound to the silica wall and prevents any significant increase in the length and aspect ratio.

In this work, we exploit a synergic effect of gaseous HF and fluorine (F_2) to improve the aspect ratio and the etching speed of microchannels fabricated by the FLICE technique. We have assembled a simple apparatus suitable to selectively etch the laser ablated zone (LAZ) with a mixture of gaseous F_2 and HF. We obtain microchannels having a significantly improved aspect ratio of 86 with a comparatively high etching speed of 17 μm min^{-1}.

1. Materials and methods

The procedure adopted comprises of two subsequent steps. First, a fused silica slab ($1 \times 2 \times 6$ mm^3) is irradiated with a femtosecond laser. Then, the irradiated sample is etched by a gaseous mixture of HF/F_2.

1.1. Femtosecond laser irradiation

The substrates used for the microchannel fabrication are $1 \times 2 \times 6$ mm^3 slabs made up of commercial fused silica (Foctek Photonics, China). The experimental setup used for the laser irradiation process is shown in figure 1. It starts with a regeneratively amplified Ti: sapphire laser (model CPA-1 from Clark Instrumentation), generating 150 fs, 500 μJ pulses at 1 kHz repetition rate and 790 nm wavelength. For the irradiation, we use only a fraction of the pulse energy, up to 5 μJ. The beam, initially with circular cross section, is astigmatically shaped by passing it through a cylindrical telescope ($f1 = 50$ mm, $f2 = 150$ mm), thus providing a demagnification by a factor 3 in one transverse direction. Astigmatic beam shaping allows us to control the focal volume in such a way that the cross section of the modified track becomes symmetric and with arbitrary size [21]. The astigmatically shaped beam is focused by a 50× microscope objective (numerical aperture 0.6, focal length 4 mm). The writing beam polarization is linear and orthogonal to the translation direction. The samples are moved perpendicularly to the beam propagation direction by a precision translation stage (Physik Instrumente) at a constant speed [22].

1.2. Iterative etching using a mixture of HF and F_2

A scheme of the experimental setup used for the gaseous etching is shown in figure 2. It derives from a similar apparatus that we developed in a previous study [15, 16, 23]. The setup was built using fluorine resistant alloys with 1/4 in. AISI316 tubing and AISI316 severe service valves (Swagelok JB and JBR), according to the procedures for safety handling of HF described in the literature [24]. The gases used are anhydrous HF (>99.5%) from Rivoira, F_2 from Solvay Fluor (98%) and nitrogen. The reactor is an AISI316 1/4 in. tube with 1/16 in. and 1/8 in. connections, it has a volume of 52 cm^3 and is connected with a stainless steel membrane to a pressure measurement system (Endress+Hauser Cerabar

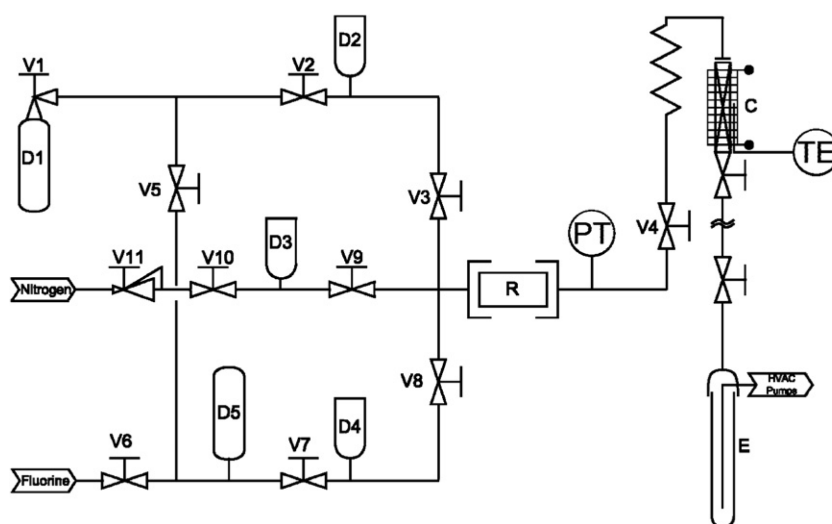

Figure 2. Schematic of the etching apparatus. D1: hydrofluoric acid cylinder; D2, D3, D4: expansion drums; D5: HF/F_2 cylinder V1–V11: valves; R: etching reactor; C: heated soda lime trap; E: liquid nitrogen cooled trap; PT: pressure transducer; TE: thermocouple.

T PMP131). The reactor is also connected through the vacuum line to a knock-out trap and a liquid-nitrogen cooled condenser that sequestrates the unreacted gases and moisture, hence protecting the vacuum pumps. The knock-out trap is a 2×50 cm^2 glass tube limited by two valves and filled with soda lime that contains ethyl-violet in order to provide a visual measurement of the soda consumption. The unreacted HF and F_2 present in the etching gases react exothermically with the soda lime. The trap is heated once a day using an electric sheath to 230 °C for 2 h to release most of the absorbed water derived from the reaction of HF and F_2 with soda lime. This water is frosted in the liquid-nitrogen cooled condenser and subsequently disposed. Vacuum in the reactor (1×10^{-4} mbar) is provided by the combination of two pumps: a rotative pump (Boc Edwards RV12) and a diffusive pump (Boc Edwards 8000 L h^{-1}).

The irradiated fused silica sample is loaded in the reactor and the tube is connected to the vacuum line. Subsequently, the etching mixture is prepared in cylinder D5 by acting on valves V5 and V6. The total pressure inside the cylinder D5 is between 1.0 and 1.5 bar. The reactor is first put under vacuum and then filled with the etching mixture at the selected pressure (P_{mix}) and room temperature using the vacuum line limited by the two valves V7–V8.

After the desired reaction time t_R, the reactor is connected to the vacuum line and the unreacted gases, as well as the reaction products, are removed. Subsequently, the reactor is reconnected to the etching gas reservoir (by closing V4 and opening V8) and the cycle is repeated for a given number of times until the desired channel length is obtained. A complete cycle consists of the combination of two steps: (1) gas-fused silica reaction and (2) products desorption. For all experiments, the desorption time t_D has been fixed to 10 min to completely evacuate the reactor.

After the desired number of cycles has been executed, the system is purged with vacuum and subsequently with nitrogen. The reactor is opened and the length and diameter of the etched channels are measured by a polarized light microscope (Olympus BX51).

1.3. Safety

Fluorine and gaseous HF [24, 25] should be handled with extreme care. Pure fluorine is heavier than air and reacts quickly with water to form hydrogen fluoride and with unpassivated steel or dirt equipment. The pressure inside the hydrogen fluoride storage cylinder should be monitored frequently because hydrogen is produced by the reaction between HF and the metallic wall of the storage cylinder. The hydrogen formed reacts with fluorine thus changing the F_2/HF ratio; therefore, HF used should be purified frequently.

2. Results and discussion

The known etching of irradiated fused silica with pure HF, both in the liquid and gaseous phases, results in limited channel lengths and aspect ratios because it is very difficult to replace the reacted HF inside the microchannel. In addition, water is formed during the HF action on silica, and this etching product further dilutes the HF acid and causes even more impediments to the HF diffusion along the channel. The added F_2, although not directly participating in the silica etching reaction, provides an *in situ* regeneration of HF, thus increasing the etch speed and aspect ratio even in long channels, as described below.

The overall reaction between silica and F_2 is shown in scheme 1. It is highly exothermic [26] (-716 kJ mol^{-1}) with an increase of entropy (40.8 J mol^{-1} K^{-1}):

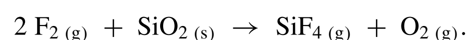

$$2\,F_{2\,(g)} + SiO_{2\,(s)} \rightarrow SiF_{4\,(g)} + O_{2\,(g)}.$$

Scheme 1: Overall etching reaction using fluorine. Subscripts indicate the phase. $_{(s)}$: solid. $_{(g)}$: gas.

Despite the favorable thermochemical state, pure F_2 needs traces of water or hydrogen fluoride to initiate the etching reaction at room temperature and low pressure [27]. Water is formed in the first reaction of scheme 2 along with silicon tetrafluoride. Water, as shown in reaction 2, reacts vigorously with fluorine forming unstable oxyfluorides [27–31] that rapidly decompose into hydrogen fluoride and oxygen:

Figure 3. Top: prolate spheroid-like channel obtained with 40-120 procedure. Bottom: conical channel obtained with 20-20 procedure.

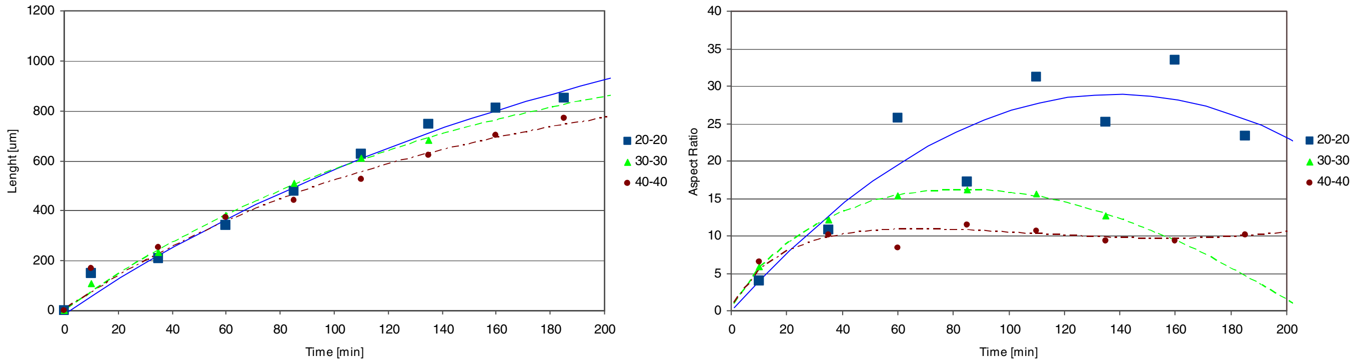

Figure 4. Etching kinetics of tests 20-20, 30-30 and 40-40. Left: length versus time fitted using scheme 3. Right: aspect ratio versus time with a guide to the eye.

Table 1. Experimental results in the etching of SiO_2 with gaseous mixture of HF/F_2 at room temperature and different partial pressure. P_{HF}: hydrogen fluoride partial pressure. P_{F_2}: fluorine partial pressure. $P_{HF} + P_{F_2}$: total pressure. t_R: reaction time. t_D: vacuum time. U.L.: saturation length. M.A.R.: maximum aspect ratio. $L_{(M.A.R.)}$: length evaluated at the maximum aspect ratio. I.E.S.: initial etching speed.

Name	P_{HF} (mbar)	P_{F_2} (mbar)	$P_{HF} + P_{F_2}$ (mbar)	t_R (min)	t_D (min)	U.L. (μm)	M.A.R. (−)	$L_{(M.A.R)}$ (μm)	I.E.S (μm min^{-1})
40-120	40	120	160	5	10	1273.2	18.4	784.6	9.5
40-80	40	80	120	5	10	1342.5	15.0	499.7	10.4
30-60	20	40	60	5	10	1443.5	19.6	966.9	7.4
40-40	40	40	80	5	10	1005.5	10.9	407.6	12.5
30-30	30	30	60	5	10	1166.8	16.2	484.8	7.9
20-20	20	20	40	5	10	1518.0	28.9	732.8	7.4
6-14	6	14	20	2	3	1622	86	1205	30

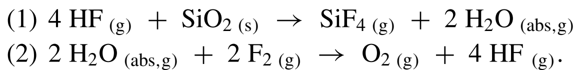

Scheme 2: Model proposed. The water formed in reaction 1 is used in reaction 2, thus providing a mechanism for the *in situ* regeneration of HF. Subscripts indicate the phase. $_{(s)}$: solid. $_{(g)}$: gas. $_{(abs,g)}$: absorbed gas on the channel walls.

The water initially adsorbed on the microchannel walls migrates toward the outside environment. However, in the second step, the presence of F_2 converts the water back to HF, thus providing a supply of fresh etchant.

This mechanism is responsible for the *in situ* regeneration of HF etching reagent that reacts with silica. To validate this mechanism we have performed several etching tests. The overall results including aspect ratio, ultimate length and initial etching speed are reported in table 1.

The *aspect ratio* is defined as the ratio between the length of the microchannel and its diameter measured at the surface. This definition fitted perfectly with the data of our previous work [15]. However, as shown in figure 3, in our experiments the channel shapes obtained vary and the maximum diameter is not the one measured on the surface. Thus, the aspect ratio reported in this work is the coefficient calculated by relating the length of the microchannel to the maximum diameter of the channel, which in some tests (figure 3) does not coincide with the diameter measured on the surface.

The fitting of the experimental data shown in figures 4, 5 and 8 has been carried out by using the appropriate mathematical model described in scheme 3.

Scheme 3: Model used for data fitting. *A*, *B*, *C*,: adaptive parameters. *t*: time.

$$\text{Length}(t) = A + B \cdot e^{-C \cdot t}.$$

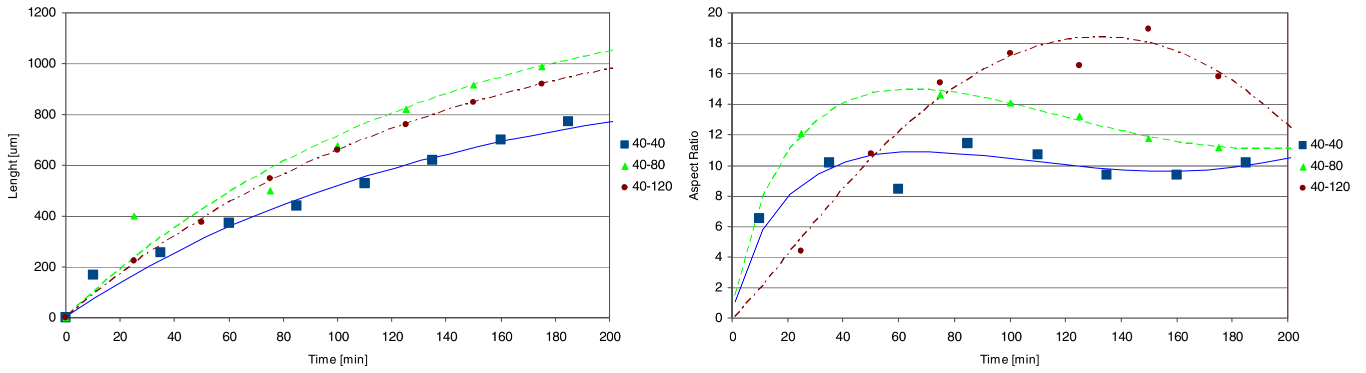

Figure 5. Etching kinetics of tests 40-40, 40-80 and 40-120. Left: length versus time fitted using scheme 3. Right: aspect ratio versus time with a guide to the eye.

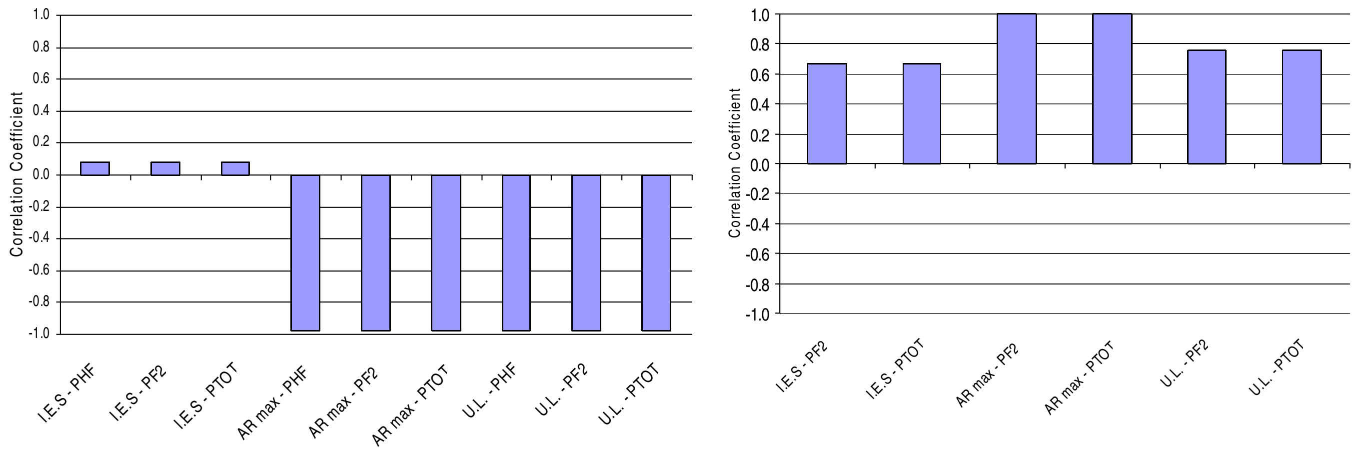

Figure 6. Left: correlation factors calculated for tests 20-20, 30-30 and 40-40. Right: correlation factors calculated for tests 40-40, 40-80 and 40-120. I.E.S.: initial etching speed. A.R.: aspect ratio. U.L.: saturation length. PHF: hydrogen fluoride pressure. PF2: fluorine pressure. PTOT: sum of fluorine pressure and hydrogen fluoride pressure.

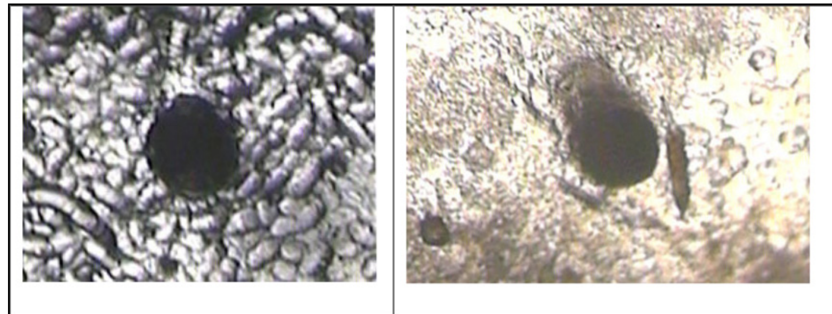

Figure 7. Side view of the holes in samples 40-80 (left) and 40-40 (right) taken at 200 $\times$ magnification. 40-40 sample is slightly tilted.

The etching kinetics shown in figures 4, 5 and 8 fit well with the exponential trend-line. The mathematical model of scheme 3 is derived from a diffusion equation based on the hypothesis that the reactants diffusion is slow compared to the chemical reaction ratio [15]. The first data point does not fit with the model; this is due to the shortness of the channel; indeed, in these conditions the experimental kinetic does not follow a diffusion-limited chemical reaction.

The *saturation length* and the *maximum aspect ratio* reported in table 1 were calculated from the model in scheme 3.

The *initial etching speed* is the time derivative of the length, namely the etching speed, evaluated at zero channel length.

To better understand the influence of the parameters on the *aspect ratio*, *saturation length* and *initial etching speed* of the obtained channels, the correlation factors plotted in figure 6 have been calculated using the Pearson product–moment correlation coefficient formula.

The overall calculated correlation factors in figure 6 suggest that the *initial etching speed*, the *saturation length* and the *aspect ratio* could be increased by lowering the pressure of hydrogen fluoride. In particular, in tests 20-20, 30-30 and

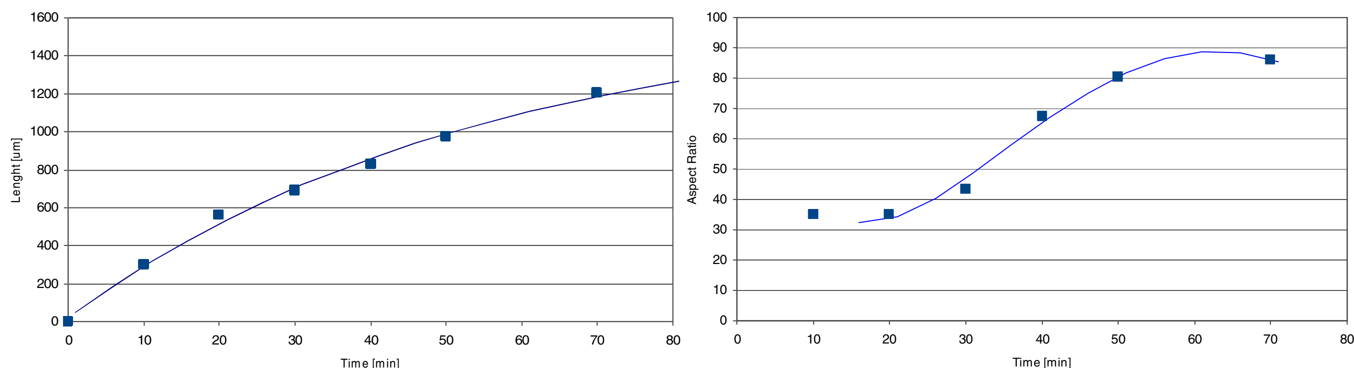

Figure 8. Etching kinetics of test 6-14. Left: length versus time fitted using scheme 3. The first data point was not fitted because it does not follow a diffusion-limited reaction. Right: aspect ratio versus time with a guide to the eye.

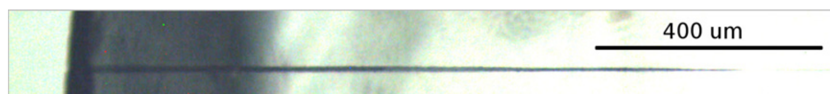

Figure 9. Microchannel obtained in test 6-14. $F_2/HF = 2.38$. $P_{HF} + P_{F_2} = 20$ mbar. $t_R = 2$ min. $t_D = 3$ min.

40-40 (central plot), where the relative amount of fluorine and hydrogen fluoride is 1:1 v/v, the aspect ratio and the etching speed increase by lowering the total pressure. This behavior is consistent with a diffusion-limited etching reaction since the diffusivity coefficient decreases by raising the pressure [32].

By raising the fluorine pressure, the initial etching speed increases and the aspect ratio seems to decrease not monotonically. Three tests at rising fluorine content, 40-40, 40-80 and 40-120, respectively, were performed to better understand the influence of fluorine on the etching reaction. The kinetic data of these tests, reported in figure 5, suggest that the aspect ratio generally increases with the increase of fluorine amount. This behavior seems to violate the hypothesis of a diffusion-driven reaction. However, it should be noted that the diffusivity of the etchant depends also on its composition: the higher the F_2/HF ratio, the higher the overall diffusion coefficient and the higher the aspect ratio.

The chemical model proposed in scheme 2 explains the synergic effect between fluorine and hydrogen fluoride in the chemical etching of silicon dioxide. It consists of two subsequent steps: the etching reaction and the hydrogen fluoride regeneration. During the experiments with a high amount of fluorine we have observed that the shape of the etched channel is a prolate spheroid. This is a clear indication that the etching of the walls is a secondary reaction activated by the HF regeneration. An etching test performed using only fluorine at low pressure did not result in any channel formation.

The etchant regeneration step described in reaction 2 of scheme 2 is the key factor to obtain cylindrically shaped channels. When the regeneration of hydrogen fluoride occurs at the bottom of the channel there is an increase of the aspect ratio. However, if water migrates away from the LAZ, then an excess of etchant is produced in the channel due to reaction with fluorine. This hydrogen fluoride cannot reach the LAZ because of its poor diffusivity, thus it reacts with the near microchannel walls. Since reaction 2 in scheme 2 is subsequent to reaction 1, we should expect a maximum aspect ratio at an appropriate reaction time.

The side view of the slabs confirms the circular shape of the cross section. Thus, the etching procedure presented herein does not influence the inlet geometry which is mainly affected by laser irradiation parameters. However, deviations from the observed behavior may not be excluded 'ex ante' because in our particular setup the pressure gradient is parallel to the glass slab and perpendicular to the channel inlet [15]; thus, it acts uniformly on the slab side.

The test labeled 6-14 in table 1 has been carried out keeping in mind all the considerations stated above. In particular, the length of the channel depends inversely on the pressure and the aspect ratio depends directly on the fraction of fluorine in the etchant and inversely on the reaction time. In this test, the reaction time and pressure were kept low and the etching mixture was enriched with fluorine in a ratio $F_2/HF = 2.38$.

The microchannel obtained in test 6-14, shown in figure 9, has an outstanding aspect ratio of 86 and, as plotted in figure 8, it was etched at a speed of 17 μm min^{-1} (average on the first 1205 μm). The saturation length achievable should be 1620 μm; however, the test performed did not approach this value.

2. Conclusions

In this paper, we have presented an improved version of the FLICE technique using a gaseous etching mixture. The synergic activation between gaseous hydrogen fluoride and pure gaseous fluorine allowed us to obtain microchannels with a remarkable aspect ratio of 86 at a corresponding etching speed of 17 μm min^{-1}. In comparison, the use of gaseous hydrogen fluoride in the FLICE technique allows us to obtain channels with an aspect ratio higher than 29 and a self-terminating length of 3 mm. The side view of the slabs confirms the circular shape of the cross section, but this result could be influenced by the relative direction of the pressure gradient and the silica slab.

We believe that this iterative gas-phase HF/F_2 etching methodology can significantly enhance the performance of the FLICE technique and may expand its field of application; indeed, the setup used can be easily automated and scaled up to the industrial application.

References

[1] Venturini F, Navarrini W, Famulari A, Sansotera M, Dardani P and Tortelli V 2012 *J. Fluorine Chem.* **140** 43–48

[2] Madou M J 2011 *Fundamentals of Microfabrication and Nanotechnology* 3rd edn (Boca Raton, FL: CRC Press) p 670

[3] Sansotera M, Bianchi C L, Lecardi G, Marchionni G, Metrangolo P, Resnati G and Navarrini W 2009 *Chem. Mater.* **21** 4498–504

[4] De Marco C, Eaton S M, Suriano R, Turri S, Levi M, Ramponi R, Cerullo G and Osellame R 2010 *ACS Appl. Mater. Interfaces* **2** 2377–84

[5] Navarrini W, Diamanti M V, Sansotera M, Persico F, Menghua W, Magagnin L and Radice S 2012 *Prog. Org. Coat.* **74** 794–800

[6] Ville K 2009 *Practical MEMS: Design of Microsystems, Accelerometers, Gyroscopes, RF MEMS, Optical MEMS, and Microfluidic Systems* (Small Gear Publishing)

[7] Gattass R R and Mazur E 2008 *Nature Photon.* **2** 219–25

[8] Khan Malek C G 2006 *Anal. Bioanal. Chem.* **385** 1351–61

[9] Khan Malek C G 2006 *Anal. Bioanal. Chem.* **385** 1362–9

[10] Yu X, Liao Y, He F, Zeng B, Cheng Y, Xu Z, Sugioka K and Midorikawa K 2011 *J. Appl. Phys.* **109** 053114

[11] Marcinkevicius A, Juodkazis S, Watanabe M, Miwa M, Matsuo S, Misawa H and Nishii J 2001 *Opt. Lett.* **26** 277–9

[12] Maselli V, Osellame R, Cerullo G, Ramponi R, Laporta P, Magagnin L and Cavallotti P L 2006 *Appl. Phys. Lett.* **88** 191107

[13] Osellame R, Maselli V, Vazquez R M, Ramponi R and Cerullo G 2007 *Appl. Phys. Lett.* **90** 231118

[14] Kiyama S, Matsuo S, Hashimoto S and Morihira Y 2009 *J. Phys. Chem.* C **113** 11560–6

[15] Venturini F, Navarrini W, Resnati G, Metrangolo P, Vazquez R M, Osellame R and Cerullo G 2010 *J. Phys. Chem.* C **114** 18712–6

[16] Venturini F, Sansotera M, Vazquez R M, Osellame R, Cerullo G and Navarrini W 2012 *Micromachines* **3** 604–14

[17] Kern W 1990 *J. Electrochem. Soc.* **137** 1887

[18] Torek K 1995 *J. Electrochem. Soc.* **142** 1322

[19] Reinhardt K A and Kern W (ed) 2008 *Handbook of Silicon Wafer Cleaning Technology* 2nd edn (Norwich, NY: William Andrew)

[20] Riva M, Pittroff M, Schwarze T, Oshinowo J and Wieland R 2009 *Solid State Technol.* **52** 20–24

[21] Osellame R, Taccheo S, Marangoni M and Ramponi R 2003 *J. Opt. Soc. Am.* B **20** 1559

[22] Hnatovsky C, Taylor R S, Simova E, Rajeev P P, Rayner D M, Bhardwaj V R and Corkum P B 2006 *Appl. Phys.* A **84** 47–61

[23] Venturini F, Sansotera M, Osellame R, Cerullo G and Walter N 2012 *Chim. Oggi-Chem. Today* **30** 10–12

[24] CDC—The National Institute for Occupational Safety and Health (NIOSH) 2011 www.cdc.gov/niosh/

[25] Walters D B 1980 *Safe Handling of Chemical Carcinogens, Mutagens, Teratogens, and Highly Toxic Substances* vol 1 (Ann Arbor, MI: Ann Arbor Science Publishers) p 406

[26] NIST 2011 *NIST Chemistry WebBook* http://webbook.nist.gov/chemistry/

[27] Bartlet N 2001 *The Oxidation of Oxygen and Related Chemistry (Selected Papers of Neil Bartlett)* (Singapore: World Scientific Publishing) p 624

[28] Booth H S (ed) 1939 *Inorganic Syntheses* vol 1 (New York: McGraw-Hill) p 194

[29] Rozen S 2005 *Eur. J. Org. Chem.* **2005** 2433–47

[30] Venturini F, Sansotera M and Navarrini W 2013 *J. Fluorine Chem.* **155** 2–20

[31] Corvaja C, Farnia G, Formenton G, Navarrini W, Sandona G and Tortelli V 1994 *J. Phys. Chem.* **98** 2307–13

[32] Perry R H and Green D W 1997 *Perry's Chemical Engineers' Handbook* 7th edn (New York: McGraw-Hill) p 2640